VAPORIZATION OF COMET NUCLEI: LIGHT CURVES AND LIFE TIMES

JOHN J. COWAN
Harvard-Smithsonian, Center for Astrophysics, Cambridge, Mass., U.S.A.
and
MICHAEL F. A'HEARN
Astronomy Program, University of Maryland, College Park, Maryland, U.S.A.

(Received 22 January, 1979; in revised form 16 March, 1979)

Abstract. We have examined the effects of vaporization from the nucleus of a comet and show that a latitude dependence of vaporization can, in some cases, explain asymmetries in cometary light curves. We also find that a non-uniform distribution of solar radiation over a comet can considerably shorten the vaporization lifetime compared to the results normally obtained by assuming that the nuclear surface is isothermal.

Independent of any latitude effects, comets with CO_2-dominated nuclei and with perihelion distances less than 0.5 AU have vaporization lifetimes less than or comparable to their dynamical ejection times. This may explain the observed deficit of comets with small perihelion distances. Similarly comets with CO_2-dominated nuclei and perihelia near Jupiter's orbit have vaporization lifetimes that are shorter than the time for capture into short-period orbits. We suggest, therefore, that at least some new comets are composed in large part of CO_2, while only H_2O-dominated comets, with lower vaporization rates, can survive to be captured into short-period orbits.

1. Introduction

The vaporization of ices in the solar system has been considered by many authors in a variety of contexts. Although the vaporization of icy particles is relevant to the formation of the solar system and to the outer planets, perhaps the most obvious application is in comets. Calculations of ice vaporization are needed to estimate the non-gravitational forces on comet nuclei (e.g., Marsden *et al.*, 1973), to explain the variation with heliocentric distance of molecular production rates and/or of brightness (e.g., A'Hearn *et al.*, 1977; or Mendis and Brin, 1978), to explain the photometric behavior of the 'dust' component of the cometary coma (e.g., Delsemme and Miller, 1971), and to determine the lifetimes of cometary nuclei (e.g., Weissman, 1977a; Lebofsky, 1975) which in turn are needed to estimate required capture rates into short-period orbits.

The present work was initially undertaken in an attempt to explain the observed variation in molecular production rates with heliocentric distance. In the course of the work, it became clear that factors omitted from some of the previous vaporization calculations could have important effects on the calculation of cometary lifetimes and other cometary parameters such as non-gravitational effects and on asymmetries in the light curves. In the present paper we examine the effects of vaporization from the nucleus of a comet. In a subsequent paper we address the vaporization from icy grains in the cometary coma in

The Moon and the Planets **21** (1979) 155–171. 0165–0807/79/0212–0155 $02.55.

order to explain the variation in molecular production rates observed for Comet West (1975n = 1976 VI).

2. Calculations

The equations describing the vaporization from a surface have been given by many authors extending back to Watson *et al.* (1963), and we repeat them here only for reference. The energy balance equation is

$$F_0(1 - A_V)r_H^{-2}\,\overline{\cos\theta} = (1 - A_{IR})\sigma T^4 + Z(T)L(T), \tag{1}$$

where F_0 is the solar constant, A_V the effective albedo for absorption of sunlight (basically the visual albedo), r_H the heliocentric distance, $\overline{\cos\theta}$ the effective projection factor for the surface, A_{IR} the effective albedo for thermal emission (basically infrared), T the surface temperature, σ the Stefan–Boltzmann constant, $Z(T)$ the vaporization rate, and $L(T)$ the latent heat of vaporization. The vaporization rate is normally given in terms of the equilibrium vapor pressure, at least for pure ices, as

$$mZ(T) = p(T)\left(\frac{m}{2\pi kT}\right)^{1/2}, \tag{2}$$

where m is the molecular weight and $p(T)$ is the equilibrium vapor pressure (vide Delsemme and Miller, 1971, for further discussion). If $p(T)$ and $L(T)$ are known from laboratory data, it is a straightforward matter to solve Equations (1) and (2) numerically for any chosen albedos and heliocentric distance.

In this work we have chosen only two substances as possible cometary nuclei: carbon dioxide ice and clathrate hydrate ice. It has been suggested that at least some parabolic comets might be composed in large part of dry ice, i.e., carbon dioxide, both on the basis of the observed variation of vaporization rates with heliocentric distance (A'Hearn *et al.*, 1977; A'Hearn and Cowan, in preparation) and on the basis of the observed abundances of carbon in several comets (Delsemme, 1977, and references therein). This suggests that dry ice might be an appropriate nuclear substance for long-period comets, at least when they are first captured into orbits of relatively large perihelion distance. The success in predicting non-gravitational effects assuming water–ice vaporization (Marsden *et al.*, 1973) suggests that water–ice, or a clathrate hydrate, is the appropriate substance to use for short-period comets. We note that some investigators (e.g., Lebofsky, 1975) have described a vaporization-rate curve for clathrates that is quite different from that of water–ice. This is due to the use of the dissociation pressure of the clathrate for the pressure, $p(T)$, in Equation (2). Delsemme and Miller (1970), however, have argued convincingly that the vaporization of the clathrate is controlled by the vaporization of the hydrate lattice so that the relevant pressure in Equation (2) is the actual vapor pressure of water. Solution of Equation (1) then differs from the case of water–ice only by a small difference in the latent heat, $L(T)$ (although one must also remember to distinguish between the $Z(T)$ from the equation, which will then refer only to the water molecules, and the total

$Z(T)$, which will include the clathrate species also). It should be noted that the surface layers will allow dissociation of the clathrate at the rate given by the dissociation pressure so that the results of Lebofsky would be correct for small particles. Although it is difficult to estimate the size at which the vaporization of the hydrate lattice would dominate, it will almost certainly dominate for the kilometer-sized bodies normally considered as cometary nuclei. Although there is good evidence for materials even more volatile than dry ice in comets (Sekanina, 1976), the indications are that this material is largely confined to a relatively thin outer layer and will therefore not be considered in this paper.

The vapor pressure of water was taken directly from Washburn (1928) as

$$\log p = \frac{-2445.5646}{T} + 8.2312 \log T - 0.016\,770\,06T + 1.205\,14 \times 10^{-5}T^2 - 6.757\,169, \tag{3a}$$

(p in mm of Hg, T in Kelvin) while that for CO_2 is taken from Egerton and Edmondson (1928) as

$$\log p = \frac{-1367.3}{T} + 9.9082 \qquad T > 138\,\text{K},$$
$$\log p = \frac{-1275.6}{T} + 0.006\,83T + 8.307 \qquad T < 138\,\text{K}. \tag{3b}$$

These vapor pressures are the same as those used by most other investigators, including Lebofsky (1975). The latent heat of vaporization of water–ice was represented by

$$L(T) = 12\,420 - 4.8T, \tag{4a}$$

(L in cal-mole^{-1}, T in Kelvin) which is a straight line fit to the data given by Delsemme and Miller (1971) while that for CO_2 ice was taken to be a constant 577 joules g^{-1} from Smith (1929). For some preliminary calculations we used

$$L(T) = 12\,160 + 0.5T - 0.033T^2, \tag{4b}$$

which is a fit to the data given by Delsemme and Miller (1971) for methane clathrate hydrate. Because graphs of this vaporization rate versus heliocentric distance showed negligible differences from the curves for pure water, we used the latent heat for water in all subsequent calculations.

A parameter which is much more difficult to evaluate is the average projection factor of the surface, $\overline{\cos\theta}$. An upper limit to the vaporization rate is given by assuming a surface normal to the incident solar radiation – i.e., $\overline{\cos\theta} = 1$. This would correspond to the sub-solar point on a slowly rotating body but would clearly not represent any sort of an average over the entire surface of a large body. A commonly used alternative approach is to assume that the surface is isothermal in which case $\overline{\cos\theta} = 0.25$. Although this is commonly referred to as the rapidly rotating case, it is certainly not that, since rapid rotation eliminates only longitudinal temperature variations while latitudinal temperature variations are still permitted. In materials of very high thermal conductivity or in very small

particles, the latitude variations can be eliminated by conduction so that the isothermal assumption can be justified, but this is certainly not the case for a kilometer-sized body with the low thermal conductivity typical of ices; and it is certainly not true for comets as evidenced by the existence of non-gravitational effects on the orbital motion. In fact, because the fraction of absorbed solar radiation which goes into vaporization (rather than thermal re-radiation) increases with temperature, the isothermal assumption sets an absolute lower limit on the effective vaporization rate. For this reason, the cometary lifetimes given by Weissman (1977a) are actually upper limits to the lifetime. Lebofsky (1975) has pointed out this problem of averaging the vaporization rate over a surface but has carried out vaporization-rate calculations only for the isothermal and non-rotating cases, and has estimated lifetimes only for the isothermal case.

In an attempt to model more realistically the vaporization of a cometary nucleus, we have assumed that the cometary nucleus rotates sufficiently rapidly that parallels of latitude are isotherms. In fact even this is not true for a typical cometary nucleus as evidenced by the fact that the non-gravitational forces acting on comets have significant transverse (non-radial) terms which require a lag angle between the point of maximum insolation and the point of maximum vaporization (vide, e.g., Marsden *et al.*, 1973). Nevertheless, we feel that our assumption does present a significant improvement over earlier work and it certainly leads to significantly different conclusions. With our assumption, another free parameter enters the calculation, viz. the angle, i, between the rotation axis and the direction to the Sun ($i = 0$ implies one pole toward the Sun while $i = \pi/2$ implies a polar axis perpendicular to the Sun–comet line). If we arbitrarily designate positive latitudes, b, as the ones in the hemisphere of the Sunward pole, the appropriate values of $\overline{\cos\theta}$ as a function of latitude are given by

$$\overline{\cos\theta} = \begin{cases} \cos i \sin b & b > +i \\ \dfrac{\cos i \sin b}{\pi} \cos^{-1}(-\tan b \cot i) + \dfrac{\sin i \cos b}{\pi} \times & \\ \times \sin[\cos^{-1}(-\tan b \cot i)] & -i < b < +i \\ 0 & b < -i. \end{cases} \tag{5}$$

We note that Sekanina (1978) has independently derived this result in a slightly different form. In order to estimate the total vaporization from a cometary nucleus with its rotation axis oriented at a particular angle i to the solar direction, we evaluate the integral

$$\overline{Z(i)} = \frac{1}{2}\int_{-\pi/2}^{\pi/2} Z(i, b) \cos b \, db, \tag{6}$$

by numerical integration after previously solving for $Z(i, b)$ at a variety of values of i and b using Equations (1) through (5). We have assumed implicitly that parameters such as albedo and composition are uniform over the surface of the nucleus even though there is evidence that, at least for a few comets such as P/Encke, there must be a variation over the surface (Delsemme and Rud, 1973; Sekanina, 1978).

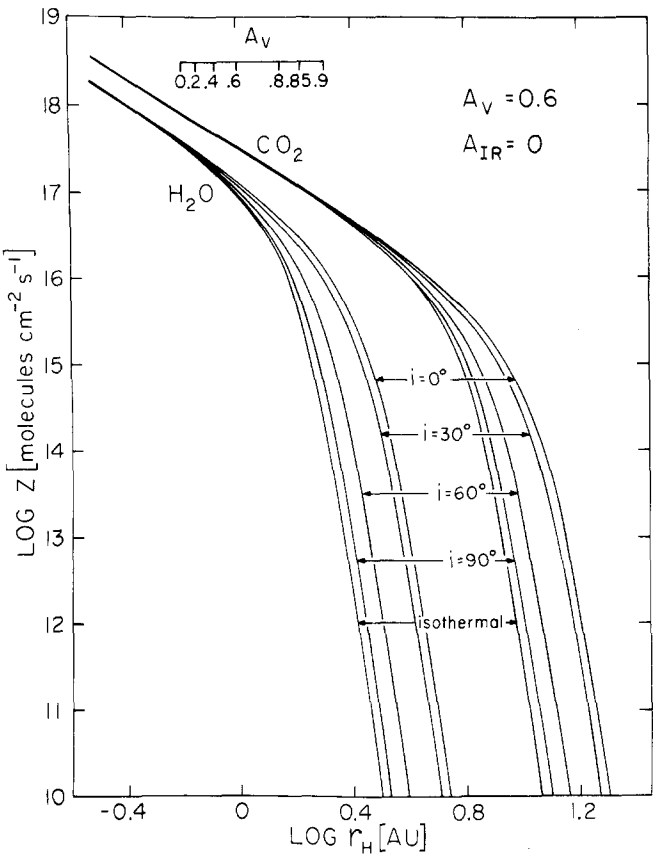

Fig. 1. Vaporization rate for H_2O and CO_2 comet nuclei as a function of heliocentric distance for visual albedo $A_V = 0.6$ and infrared albedo $A_{IR} = 0$. The inclination of the comet's rotation axis, i, is given in degrees where $i = 0°$ indicates that one pole is pointing toward the Sun, while $i = 90°$ indicates that the axis is perpendicular to the Sun–comet line. The curve for an isothermal nucleus is also shown. Curves for other visual albedos are horizontal translations of these curves, and the albedo scale at the top of the figure indicates the 1 AU point for the indicated albedos.

The calculations have been carried out, as noted above, both for dry-ice nuclei and for water–ice nuclei using a variety of different effective visual albedos but primarily for a thermal infrared albedo of 0 (unit emissivity). The results are insensitive to the infrared albedo as long as the albedo remains low. Figures 1 and 2 show the vaporization rate as a function of heliocentric distance for some typical cases. We note that the curves for other visual albedos are simply horizontal translations of these curves by an amount

$$\delta \log r = \tfrac{1}{2} \log [(1 - A)/(1 - A_0)], \tag{7}$$

where A_0 is the albedo for which the curve was initially drawn. The translation for other albedos is shown at the top of the figures. An examination of the figures shows that, if the cometary rotation axis is oriented perpendicular to the Sun–comet line ($i = \pi/2$), the resultant vaporization rate curve is only slightly different from the curve for an isother-

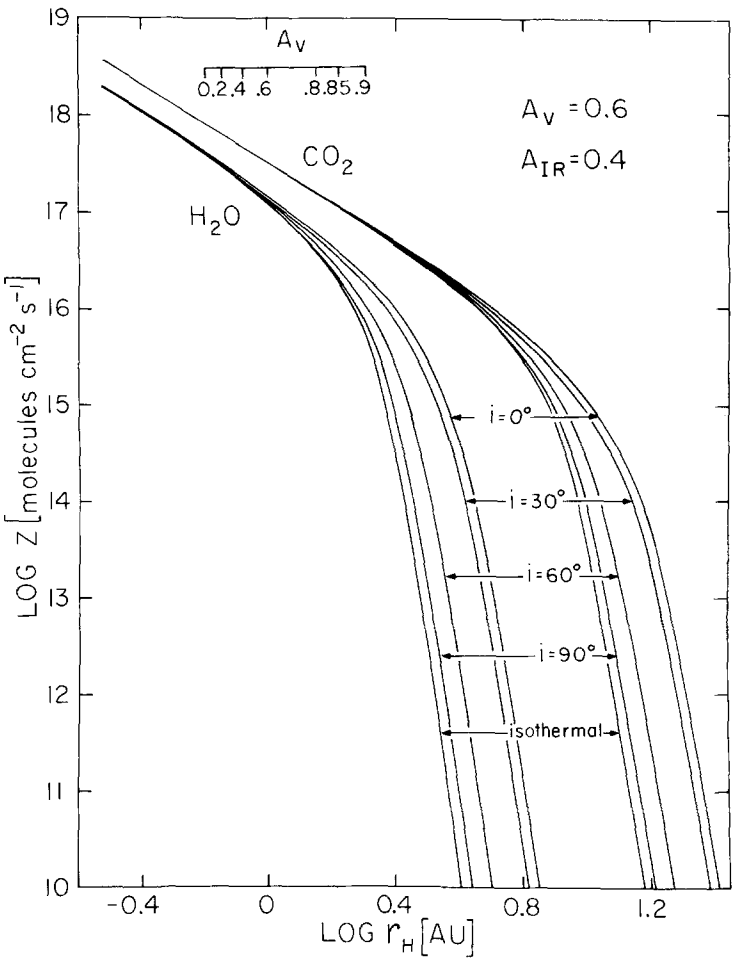

Fig. 2. Similar to Figure 1 except for an infrared albedo, $A_{IR} = 0.4$.

mal nucleus. This difference would be undetectable in most existing data. If, however, the axis is oriented parallel to the Sun–comet line (i.e., $i = 0$), the difference is quite substantial. The turnover point of the curve is moved to a significantly larger heliocentric distance. Consideration of the geometry of this latter case shows immediately that, although the result was derived for a rapidly rotating nucleus with isotherms being parallels of latitude, this result is directly applicable to the case of a non-rotating (or slowly rotating) nucleus with circular isotherms centered on the sub-solar point; i.e., a rapidly rotating nucleus with the pole toward the Sun ($i = 0$) is equivalent to a non-rotating nucleus. Since this geometry maximizes the variation of insolation across the surface of the nucleus, it represents the maximum possible vaporization rate independent of rotation-rate or surface-conductivity considerations just as the isothermal case represents the minimum possible vaporization rate independent of these considerations. As one would

expect, at small heliocentric distances the temperature is high enough that nearly all the absorbed solar radiation goes into vaporization rather than thermal re-radiation and all curves approach an r_H^{-2} dependence. The H_2O curve for $i = 0$ and $A_{IR} = 0.4$ has a turnover at nearly as large a heliocentric distance as the CO_2 curve for an isothermal nucleus and $A_{IR} = 0$. Allowance for different effective albedos will thus permit a turnover point in the vaporization curve at any heliocentric distance from 1 to 10 AU using just H_2O and CO_2. These results have implications for several studies as discussed below. We note in passing that the parameter r_0 used in modeling non-gravitational, orbital effects (Marsden *et al.*, 1973, Equation (5)) might be expected to take on a wide range of values rather than the single value $r_0 = 2.8$ AU which is normally used. This might help in improving the orbital fit to observations for some apparently anomalous comets (vide Yeomans, 1978).

3. Cometary Light Curves

It has long been known that may comets exhibit regular light curves which are not symmetrical about perihelion. One of the most notable examples is P/Encke as discussed, e.g., by Kresák (1965), but there are also many others. The present results provide a mechanism for explaining this asymmetry as a 'seasonal' effect at least in some comets. If the rotation axis of a comet lies in the orbital plane of the comet, the angle between the rotation axis and the solar direction, being equal to the true anomaly plus a constant, will change systematically as the comet moves around in its orbit. Unless the angle between the two directions is 0 or $\pi/2$ at perihelion, there will be an asymmetry in this angle about perihelion and hence an asymmetry in the vaporization rate which in turn will produce an asymmetry in the light curve. The maximum possible size of this effect can be estimated by measuring the vertical distance between the $i = 0$ and $i = \pi/2$ curves in Figures 1 and 2. This distance can exceed 3 orders of magnitude near the turn-over points of the curves and can therefore produce very large asymmetries in the light curves. Suggestions that this effect might be important go back at least 10 years (Yegibekov, 1969) but we are not aware of any detailed calculations. Furthermore, the existence of such an asymmetry in the vaporization prolonged over many perihelion passages can easily induce asymmetries in the compostion of the surface. Specifically one would expect in general that the hemisphere of the sunward pole at perihelion would have vaporized significantly more over many orbits than the other hemisphere. This would likely leave that hemisphere more covered with 'rocky' debris than the other hemisphere which would be more ice covered. Furthermore the shape of the nucleus would gradually become non-spherical.

In the specific case of P/Encke, the asymmetry in the light curve occurs at such a small perihelion distance that it cannot be explained by this effect without assuming an unrealistically high albedo. On the other hand Sekanina (1978) has shown that, at present, the rotation axis does lie nearly in the orbital plane, and Whipple and Sekanina (1978) have shown how the variation in the non-gravitational parameters of P/Encke can be explained by a precession of this pole such that it now lies nearly in the plane of the orbit. We

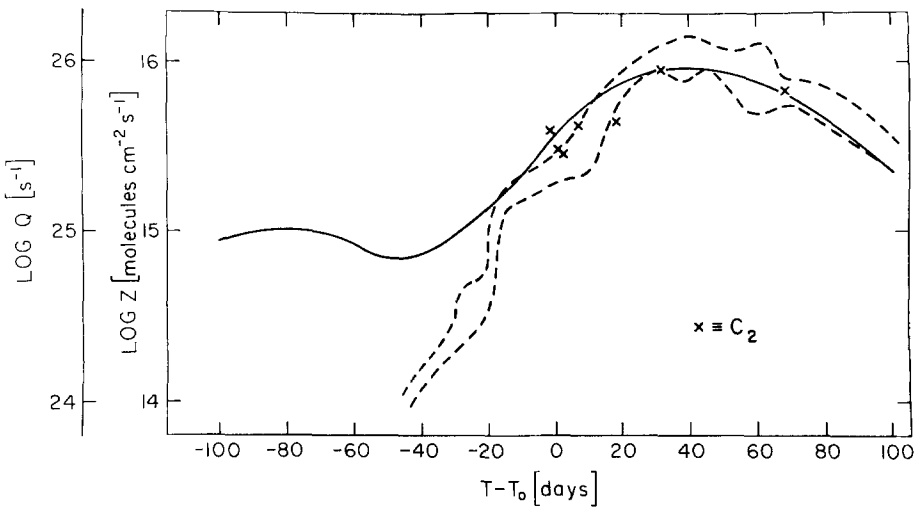

r_H [AU]	1.683	1.529	1.388	1.271	1.192	1.164	1.192	1.271	1.388	1.529	1.683
i [degrees]	144	133	120	105	86	67	47	28	13	0	11
V [degrees]	-77	-67	-54	-38	-20	0	20	38	54	67	77

Fig. 3. Perihelion asymmetry of comet P/d'Arrest. The dotted lines indicate the envelope of the determinations of visual luminosity for the 1976 apparition as collected by Bortle (1977). The symbols, X, denote C_2 production rates [radicals per second] for the 1976 apparition as measured by A'Hearn *et al.* (1979). The solid curve represents the average vaporization [molecules per cm^2 per second] for an H_2O nucleus with $A_V = 0.84$, $A_{IR} = 0$, and rotation axis in the plane of the orbit. Pole-on configuration ($i = 0°$) for this curve occurs 80 days after perihelion when the true anomaly $v = +67°$. The abscissa is labeled with the time from perihelion [days], heliocentric distance [AU], inclination of the rotation axis [degrees], and true anomaly [degrees].

suggest that the structural asymmetry, however, might originally have been set up simply by the differential vaporization from different areas on the surface of the nucleus.

Another periodic comet which shows a substantial asymmetry in its light curve is P/d'Arrest. In Figure 3 we show the observed light curve of P/d'Arrest as adapted from Bortle (1977) as well as the actual production rates of C_2 as determined by A'Hearn *et al.* (1979). We note particularly that the light curve closely follows the actual production rate of the radicals so that, at least in the case of this comet, the asymmetry cannot be related to the lifetime of the observed radicals as suggested in the model of Mendis and Brin (1978). Their mechanism can only be significant at large heliocentric distances where the lifetime of the observed species becomes comparable to the time scale over which the vaporization rate changes significantly. Furthermore, since the comet is brightest after perihelion rather than before, the asymmetry cannot be due to temporary development of a dust mantle as suggested in the model of Mendis and Brin (1977). Their later model (Brin and Mendis, 1979), in which a dust mantle is blown off, produces an asymmetry of the correct sign but with a distinctly wrong shape.

To show the effect of our mechanism, we have also plotted a theoretical vaporization rate curve for an H_2O nucleus with visual albedo 0.84 and with a rotation axis in the orbit plane with the pole-on configuration occurring 80 days after perihelion, i.e., at a true anomaly of $+ 67°$. It seems clear that the theoretical curve is capable of producing rather well the observed variation in C_2 production rates although it deviates considerably from the visual magnitude curve at times well before perihelion when it predicts that the comet should be too bright. On the other hand the discrepancy begins to become serious as the comet goes through the equator-on configuration and begins to show the 'other' hemisphere to the Sun. One would expect that repeated perihelion passages with the observed asymmetry in production rates would have produced significant hemispheric asymmetries in albedo, degree of ice cover, dust mantling, etc.

It should be pointed out that the present solution is hardly unique. There are other combinations of visual and infrared albedos and axis inclinations which can reproduce the limited amount of data on production rates. Furthermore, inclusion of hemispheric asymmetries as suggested by Whipple and Sekanina (1978) for P/Encke, will likely be necessary for all short-period comets which have had many apparitions. Nevertheless, it seems clear that simple allowances for the latitude dependence of vaporization can play a very important role in explaining cometary brightness asymmetries.

4. Cometary Lifetimes

The lifetime of comet nuclei against total destruction by vaporization is of great importance in understanding both the distribution of long-period cometary orbits and also the evolution of comets from long-period into short-period orbits. Lifetimes against ice vaporization have been calculated by Lebofsky (1975) for a variety of ices in short-period orbits while lifetimes have been calculated by Weissman (1977a) for water–ice nuclei in long-period (parabolic) orbits. Although Lebofsky has pointed out the problem of averaging the vaporization rate over latitude, neither of the above authors has taken this factor into account in his lifetime calculations. It is clear, however, from an examination of Figures 1 and 2, that the averaging over latitude can have important effects on the lifetime. This will be especially true for comets with perihelion distances comparable to the distance of the turnover point in Figures 1 and 2, but even for comets with smaller perihelion distances this effect can be important if, e.g., the comet is nearly pole-on to the Sun when it is at the distance of the turnover point.

In order to determine more realistic lifetimes, we have carried out straightforward, numerical integrations of the average vaporization rates as a function of time in a variety of cometary orbits. We have considered primarily parabolic orbits of various perihelion distances since these are by far the simplest to calculate but we have also integrated over the orbits of some real short-periodic comets, viz. P/Encke ($q = 0.34$ AU, $e = 0.85$) and P/Chernykh ($q = 2.57$, $e = 0.59$) (where q is the perihelion distance and e the eccentricity), to determine the extent to which results for elliptical orbits will differ from those for parabolic orbits. We also compared comets with parabolic orbits to those with

circular orbits. The ratio of the lifetime of comets with parabolic orbits to the lifetimes of comets with circular orbits for perihelion distances of 0.1–0.5 AU was approximately 1.8–2.8. In all cases the integrations were done with a constant step size of one day from perihelion until the daily vaporization was less than 10^{-6} of the integral vaporization. For water nuclei in parabolic orbits with the variety of albedos that we considered, the end point of the integrations occurred at heliocentric distance of approximately 2–7 AU, while for CO_2 nuclei the end point range was approximately 6–20 AU.

The results are presented in Tables I–IV in terms of the total mass vaporized per perihelion passage per cm^2 of nuclear surface. In order to convert these numbers to lifetimes, we have assumed an initial radius of 1 km and a uniform nuclear density of 0.5 g cm^{-3} and we have assumed that the direct vaporization from the nucleus constitutes all the mass loss. The lifetimes can be scaled directly for other densities and initial radii. It is also likely, as suggested by Delsemme and Miller (1971), that an icy grain halo is dragged out by the outflowing gas and that the mass of grains dragged out is comparable to the mass of gas. This would imply that the total mass loss from the cometary nucleus is roughly twice what we have calculated, a factor which can also be used directly to scale the lifetimes. The lifetimes for H_2O with $A_V = 0.6$ and $i = \pi/2$ agree well with the corresponding results of Weissman (1977a) for an isothermal nucleus (see Table V).

The first interesting result from these calculations is the not very surprising one that that difference in total vaporization between elliptical and parabolic orbits is small. This can be seen most easily in Figure 4 where we have plotted points corresponding to the actual orbits of P/Encke and P/Chernykh as well as the corresponding points for parabolic orbits of the same perihelion distance. The differences are not negligible but they are small compared to the differences produced by considering other effects and we will therefore not consider elliptical orbits any further.

The importance of rotation in distributing the solar insolation around the surface is also clearly seen in Figures 4 and 5 and Table V. Recalling that an inclination of 0 is equivalent to a very slowly rotating nucleus, the difference between rapidly and slowly rotating nuclear lifetimes is quite substantial; the curves for different inclinations diverging as the perihelion distance increases. In particular, water-ice nuclei with $A_V = 0.8$ and $A_{IR} = 0$ show a variation by a factor of 4 in lifetime for a perihelion distance of 1.0 AU and a variation by a factor of 60 for 1.5 AU. The differences for CO_2 nuclei are small for these perihelion distances but become substantial at perihelion distances of several AU, i.e., at the distance of Jupiter's orbit, the region from which short-period comets may be captured.

We have run a few cases, also given in Table V, in which the rotation axis is in the plane of the orbit but fixed in space so that the inclination angle varies with the true anomaly. As expected, these cases lie intermediate between the zero and $\pi/2$ inclinations which represent nearly the extreme possible cases since the isothermal case has only a slightly lower vaporization, hence slightly longer lifetime, than the $\pi/2$ inclination case. These cases with the rotation axis in the plane of the orbit can lie close to either extreme depending on where in the orbit the rotation axis points towards the Sun.

Table I

Mass loss per orbit [gm cm^{-2}] for H_2O nuclei. Inclination = $\pi/2$

Albedos		Perihelion distance [AU]						
A_V	A_{IR}	0.1	0.3	0.5	1.0	1.5	2.0	3.0
0.4	0	4.214×10^{2}	1.886×10^{2}	1.153×10^{2}	4.128×10^{1}	1.281×10^{1}	2.274	5.638×10^{-3}
0.4	0.2	4.288×10^{2}	1.967×10^{2}	1.239×10^{2}	4.942×10^{1}	1.897×10^{1}	5.37	5.138×10^{-2}
0.4	0.4	4.376×10^{2}	2.062×10^{2}	1.338×10^{2}	5.946×10^{1}	2.752×10^{1}	1.114×10^{1}	5.574×10^{-1}
0.6	0	2.72×10^{2}	1.161×10^{2}	6.692×10^{1}	1.872×10^{1}	3.24	1.464×10^{-1}	6.784×10^{-1}
0.6	0.2	2.776×10^{2}	1.222×10^{2}	7.324×10^{1}	2.42×10^{1}	6.298	7.312×10^{-1}	8.216×10^{-4}
0.6	0.4	2.84×10^{2}	1.294×10^{2}	8.074×10^{1}	3.126×10^{1}	1.13×10^{1}	2.812	1.628×10^{-2}
0.8	0	1.271×10^{2}	4.844×10^{1}	2.38×10^{1}	2.79	3.354×10^{-2}	1.41×10^{-4}	1.235×10^{-8}
0.8	0.2	1.305×10^{2}	5.216×10^{1}	2.75×10^{1}	4.9	2.114×10^{-1}	1.568×10^{-3}	2.326×10^{-7}
0.8	0.4	1.345×10^{2}	5.658×10^{1}	3.196×10^{1}	8.142	1.077	2.76×10^{-2}	8.168×10^{-6}

Table II

Mass loss per orbid [gm cm^{-2}] for H_2O nuclei. Inclination = 0 or slowly rotating

Albedos		Perihelion distance [AU]						
A_V	A_{IR}	0.1	0.3	0.5	1.0	1.5	2.0	3.0
0.4	0	4.416×10^{2}	2.116×10^{2}	1.398×10^{2}	6.636×10^{1}	3.456×10^{1}	1.75×10^{1}	3.14
0.4	0.2	4.476×10^{2}	2.18×10^{2}	1.464×10^{2}	7.318×10^{1}	4.09×10^{1}	2.288×10^{1}	5.882
0.4	0.4	4.544×10^{2}	2.254×10^{2}	1.542×10^{2}	8.136×10^{1}	4.88×10^{1}	3.0×10^{1}	1.049×10^{1}
0.6	0	2.872×10^{2}	1.336×10^{2}	8.542×10^{1}	3.644×10^{1}	1.624×10^{1}	6.47	4.232×10^{-1}
0.6	0.2	2.916×10^{2}	1.383×10^{2}	9.036×10^{1}	4.138×10^{1}	2.048×10^{1}	9.604	1.27
0.6	0.4	2.968×10^{2}	1.439×10^{2}	9.622×10^{1}	4.738×10^{1}	2.594×10^{1}	1.411×10^{1}	3.276
0.8	0	1.366×10^{2}	5.926×10^{1}	3.494×10^{1}	1.115×10^{1}	2.984	4.56×10^{-1}	1.062×10^{-3}
0.8	0.2	1.392×10^{2}	6.218×10^{1}	3.792×10^{1}	1.375×10^{1}	4.672	1.152	9.69×10^{-3}
0.8	0.4	1.423×10^{2}	6.56×10^{1}	4.15×10^{1}	1.708×10^{1}	7.182	2.594	1.065×10^{-1}

Table III

Mass loss per orbit [gm cm^{-2}] for CO_2 nuclei. Inclination = $\pi/2$

Albedos		Perihelion distance [AU]							
A_V	A_{IR}	0.1	0.3	0.5	1.0	1.5	2.0	3.0	5.2
0.4	0	9.004×10^{2}	4.74×10^{2}	3.418×10^{2}	2.07×10^{2}	1.461×10^{2}	1.093×10^{2}	6.53×10^{1}	2.056×10^{1}
0.4	0.2	9.07×10^{2}	4.808×10^{2}	3.488×10^{2}	2.144×10^{2}	1.539×10^{2}	1.173×10^{2}	7.336×10^{1}	2.734×10^{1}
0.4	0.4	9.148×10^{2}	4.888×10^{2}	3.572×10^{2}	2.234×10^{2}	1.631×10^{2}	1.268×10^{2}	8.304×10^{1}	3.618×10^{1}
0.6	0	5.926×10^{2}	3.08×10^{2}	2.196×10^{2}	1.292×10^{2}	8.832×10^{1}	6.362×10^{1}	3.442×10^{1}	7.102
0.6	0.2	5.976×10^{2}	3.132×10^{2}	2.248×10^{2}	1.349×10^{2}	9.418×10^{1}	6.956×10^{1}	4.022×10^{1}	1.109×10^{1}
0.6	0.4	6.034×10^{2}	3.192×10^{2}	2.312×10^{2}	1.415×10^{2}	1.011×10^{2}	7.664×10^{1}	4.73×10^{1}	1.68×10^{1}
0.8	0	2.888×10^{2}	1.461×10^{2}	1.015	5.578×10^{1}	3.506×10^{1}	2.274×10^{1}	9.036	2.96×10^{-1}
0.8	0.2	2.918×10^{2}	1.492×10^{2}	1.048×10^{2}	5.924×10^{1}	3.86×10^{1}	2.622×10^{2}	1.201×10^{1}	1.005
0.8	0.4	2.952×10^{2}	1.529×10^{2}	1.086×10^{2}	6.334×10^{1}	4.282×10^{1}	3.046×10^{1}	1.59×10^{1}	2.75

Table IV

Mass loss per orbit [gm cm^{-2}] for CO_2 nuclei. Inclination = 0 or slowly rotating

Albedos		Perihelion distance [AU]							
A_V	A_{IR}	0.1	0.3	0.5	1.0	1.5	2.0	3.0	5.2
0.4	0	9.138×10^{2}	4.91×10^{2}	3.602×10^{2}	2.276×10^{2}	1.681×10^{2}	1.322×10^{2}	8.904×10^{1}	4.276×10^{1}
0.4	0.2	9.19×10^{2}	4.964×10^{2}	3.658×10^{2}	2.334×10^{2}	1.742×10^{2}	1.384×10^{2}	9.546×10^{1}	4.9×10^{1}
0.4	0.4	9.252×10^{2}	5.028×10^{2}	3.724×10^{2}	2.404×10^{2}	1.813×10^{2}	1.458×10^{2}	1.031×10^{2}	5.666×10^{1}
0.6	0	6.032×10^{2}	3.21×10^{2}	$2.3\ 8 \times 10^{2}$	1.45×10^{2}	1.05×10^{2}	8.086×10^{1}	5.192×10^{1}	2.162×10^{1}
0.6	0.2	6.07×10^{2}	3.25×10^{2}	2.378×10^{2}	1.493×10^{2}	1.096×10^{2}	8.554×10^{1}	5.668×10^{1}	2.596×10^{1}
0.6	0.4	6.116×10^{2}	3.298×10	2.428×10^{2}	1.545×10^{2}	1.149×10^{2}	9.106×10^{1}	6.238×10^{1}	3.14×10^{1}
0.8	0	2.956×10^{2}	1.543×10^{2}	1.104×10^{2}	6.562×10^{1}	4.538×10^{1}	3.318×10^{1}	1.878×10^{1}	5.11
0.8	0.2	2.98×10^{2}	1.567×10^{2}	1.129×10^{2}	6.832×10^{1}	4.816×10^{1}	3.6×10^{1}	2.152×10^{1}	7.106
0.8	0.4	3.008×10^{2}	1.596×10^{2}	1.159×10^{2}	7.148×10^{1}	5.148×10^{1}	3.938×10^{1}	2.488×10^{1}	9.854

Table V

Lifetime [number of orbits] for H_2O comet nuclei with $A_V = 0.6$ and $A_{IR} = 0$

Perihelion distance [AU]	Inclination of comet's rotation axis		
	$i = \pi/2$	$i = 0$	$i = 0$ at perihelion
0.1	184	174	–
0.3	431	374	–
0.5	747	585	–
1.0	2.67×10^4	1.37×10^3	1.97×10^3
1.5	1.54×10^4	3.08×10^3	4.75×10^3
2.0	3.42×10^5	7.73×10^3	1.19×10^4
3.0	7.27×10^8	1.18×10^5	1.74×10^5

The lifetimes calculated here appear capable of explaining some of the observed anomalies in the distribution of cometary orbits. Weissman (1977b) has shown that stellar perturbations of Oort-cloud comets should lead ultimately to a distribution of perihelion distances, q, for new ($1/a_0 < 10^{-4}\,\mathrm{AU}^{-1}$) plus long period ($10^{-4} < 1/a_0 < 0.03\,\mathrm{AU}^{-1}$) comets (where a_0 is the 'original' semimajor axis) that is flat over the range $0 < q < 10\,\mathrm{AU}$. Nevertheless the observed distribution of perihelion distances is far from flat. Everhart (1967) showed that there was a deficit of comets with perihelion distance less than 1 AU which could not be accounted for by observational selection effects while an observed deficit at large heliocentric distances was probably consistent with a flat, intrinsic distribution coupled with strong, observational selection effects. More recently Marsden *et al.* (1978) have shown that the deficit at small perihelion distances is actually significant only for $q < 0.5\,\mathrm{AU}$ and that the effect is much more pronounced for the long-period comets than for the new comets. They have also shown that the deficit at large q is similarly more pronounced for long-period comets than for new comets although they have not considered the question of selection effects. In an attempt to explain the deficit of comets with small q, Weissman (1978) invoked mantle building on these comets such that vaporization of several tens of meters of ice renders the comets unobservable due to accumulation of non-volatile particles. He further required that most comets (85%) be very susceptible to disruption (12% probability per perihelion passage) on close approaches to the Sun. With these two assumptions he was able to reproduce the observed deficit of comets with small q.

As an alternative hypothesis, we propose that at least some new comets are composed of a sufficient quantity of CO_2 that it controls the vaporization from the nucleus. Evidence for significant amounts of CO_2 (or possibly CO) in at least some new comets has been presented in Delsemme (1977); and in a subsequent paper (A'Hearn and Cowan, in preparation) we will present evidence that CO_2 or a similarly volatile substance controlled the vaporization in at least one recent comet. With this hypothesis, the relatively short lifetime of CO_2 cometary nuclei can explain the observed deficit of comets with small q.

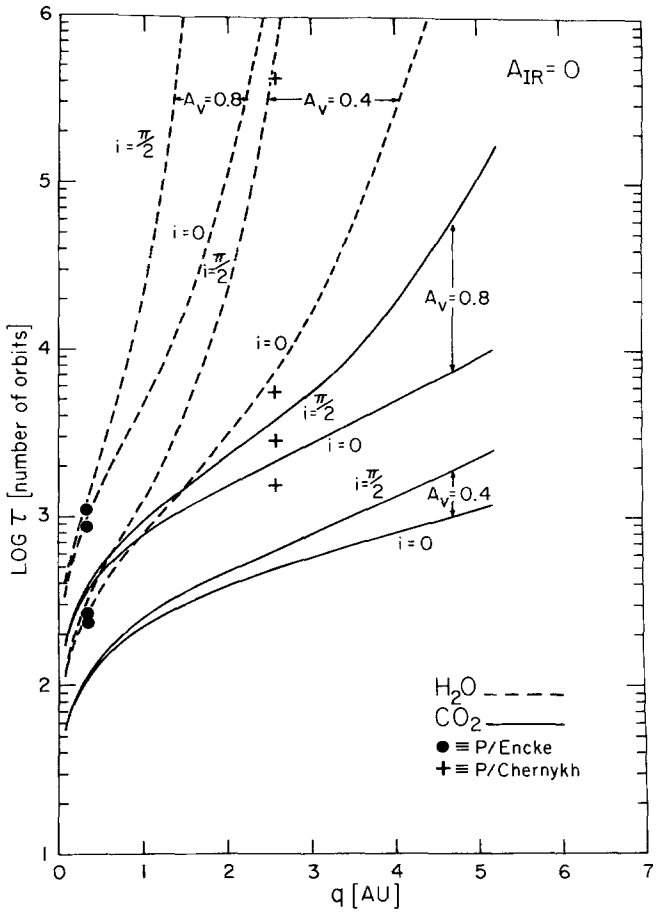

Fig. 4. Lifetimes for H_2O and CO_2 comet nuclei in parabolic orbits for visual albedos 0.4 and 0.8, inclinations $i = 0°$ and $90°$, and an infrared albedo $A_{IR} = 0$. Lifetimes are given as number of perihelion passages as a function of perihelion distance, q. The solid circles at $q = 0.34$ AU indicate results for H_2O comet nuclei in the actual elliptical orbit of comet P/Encke, while the crosses at $q = 2.57$ AU represent H_2O and CO_2 comet nuclei in the actual elliptical orbit of comet P/Chernykh. Each individual point for P/Encke and P/Chernykh should be compared with the curve immediately above it. These results indicate the shortening of lifetime to be expected for typical orbits of short period comets.

Statistical studies by Lyttleton and Hammersley (1964) and more recently by Everhart (1976) have shown that most comets (> 95%) passing through the planetary system will be gravitationally ejected from the solar system on a time scale of 50 to 100 perihelion passages (although many are ejected on the first passage and about half within 10 passages). Nuclei of CO_2 with $q < 0.5$ AU have vaporization lifetimes that are less than or comparable to the dynamical ejection time. Thus the presence of some CO_2-dominated comets could explain the deficit of comets with $q < 0.5$ AU. The deficit of all comets at large q, however, must still remain as an effect of observational selection while the

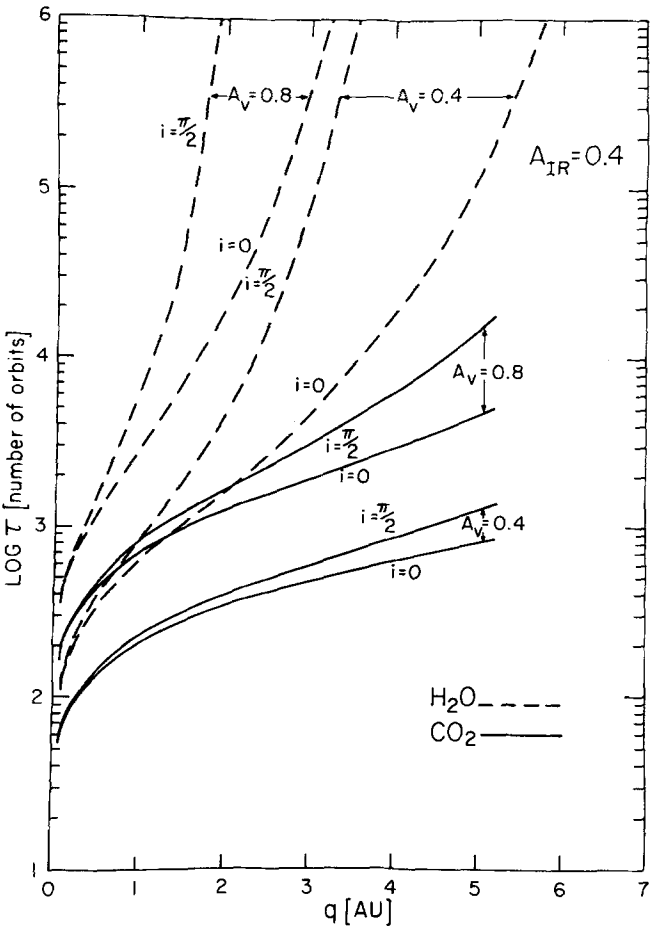

Fig. 5. Similar to Figure 4 except for an infrared albedo, $A_{IR} = 0.4$.

relatively larger effect for long-period comets might be due to fading or layering of the comets as suggested by Marsden *et al.* (1978). Note that even for $q = 3.0$ AU the vaporization of a CO_2 nucleus can amount to meters per perihelion passage.

It is also instructive to consider the lifetimes of CO_2 nuclei with perihelia near Jupiter's orbit since it has been shown by Everhart (1972, 1976) that a likely process for the capture of typical short-period comets involves an intermediate stage in which the comet has an intermediate or short period with perihelion near Jupiter's orbit, a stage during which the orbit is even likely to be circular for some time. According to Everhart a typical short-period comet can be evolved from a long-period comet with perihelion near Jupiter after a few hundred to a few thousand perihelion passages. The vaporization lifetime for a CO_2 nucleus with perihelion near Jupiter's orbit is likely to be less than a few thousand orbits based on our calculations for parabolic orbits. Any extended period of time in a nearly circular orbit will considerably shorten this lifetime as can be seen by comparing

our results with those of Lebofsky (1975) for circular orbits. The fact that this vaporization lifetime is comparable to the evolution time into short-period orbits suggests that, if some comets are primarily H_2O while others contain sufficient CO_2 for the CO_2 to control the vaporization, then there will be a strong selection effect such that only the H_2O dominated comets can be captured into short-period orbits. This might be expected to lead to systematic differences between the short period and the parabolic comets. Such differences have not heretofore been observed. A similar conclusion holds if there is a difference with depth in the nucleus rather than a difference throughout; only the portion in which H_2O dominates is likely to survive the capture process.

We finally note that lifetimes for typical short-period comets with H_2O nuclei and with perihelion distances between 0.5 and 1.0 AU are typically a few hundred to a few thousand orbits, a point which has been made previously by many authors. In particular, we note that for reasonable albedos, the observed lifetime of P/Encke (more than 50 orbits) is a significant fraction of the total vaporization lifetime (a few hundred orbits). Periodic comets of somewhat larger perihelion distance, say 1.5 AU or greater, will have H_2O vaporization lifetimes that are long compared to the time scale over which they are dynamically stable and should thus disappear solely due to dynamical effects rather than due to vaporization effects.

4. Conclusions

We have shown that the distribution of solar insolation over the surface of a rotating cometary nucleus can have important effects which should be taken into account in a variety of circumstances. In particular, large asymmetries in the light curves can, at least in some cases, be explained simply as a 'seasonal' effect due to a variation in the angle between the comet's rotation axis and the Sun–comet line. Furthermore, a non-uniform distribution of the insolation can also considerably shorten the vaporization lifetimes compared to the results more usually calculated by assuming that the nuclear surface is isothermal.

Acknowledgements

This work was supported in part by NASA grant NSG-7322 at the University of Maryland and by NASA grant NGR 22-007-269 at Harvard University. We would like to thank Brian Marsden for providing orbital information on the short period comets and Z. Sekanina for providing his results prior to publication. We have also had helpful discussions with A. H. Delsemme, H. J. Smith and P. Weissman. The numerical calculations for this paper were performed on a NOVA 3/D minicomputer. We thank A. G. W. Cameron for allowing us to use his machine for extended periods of time.

References

A'Hearn, M. F., Millis, R. L., and Birch, P. V.: 1979, *Astron. J.* **84**, 570.
A'Hearn, M. F., Thurber, C. H., and Millis, R. L.: 1977, *Astron. J.* **82**, 518.
Bortle, J. E.: 1977, *Sky and Telescope* **53**, 152.
Brin, G. D. and Mendis, D. A.: 1979, *Astrophys. J.* (in press).
Delsemme, A. H.: 1977, in A. H. Delsemme (ed.), *Comets, Asteroids and Meteorites*, University of Toledo Press, Toledo, p. 3.
Delsemme, A. H. and Miller, D. C.: 1970, *Planet. Space Sci.* **18**, 717.
Delsemme, A. H. and Miller, D. C.: 1971, *Planet. Space Sci.* **19**, 1229.
Delsemme, A. H. and Rud, D. A.: 1973, *Astron. Astrophys.* **28**, 1.
Egerton, A. C. and Edmondson, W.: 1928, in *International Critical Tables*, Vol. III, p. 207.
Everhart, E.: 1967, *Astron. J.* **72**, 1002.
Everhart, E.: 1972, *Astrophys. Lett.* **10**, 131.
Everhart, E.: 1976, in B. Donn *et al.* (eds.), *The Study of Comets*, NASA SP-393, U.S. Govt. Print. Off., Washington, D.C., p. 445.
Kresák, L.: 1965, *Bull. Astron. Inst. Czech.* **16**, 348.
Lebofsky, L. A.: 1975, *Icarus* **25**, 205.
Lyttleton, R. A. and Hammersley, J. M.: 1964, *Mon. Not. R. Astron. Soc.* **127**, 257.
Marsden, B. G., Sekanina, Z. and Everhart, E.: 1978, *Astron. J.* **83**, 64.
Marsden, B. G., Sekanina, Z. and Yeomans, D. K.: 1973, *Astron. J.* **78**, 211.
Mendis, D. A. and Brin, G. D.: 1977, *The Moon and the Planets* **17**, 359.
Mendis, D. A. and Brin, G. D.: 1978, *The Moon and the Planets* **18**, 77.
Sekanina, Z.: 1976, in B. Donn *et al.* (eds.), *The Study of Comets*, NASA SP-393, U.S. Govt. Print. Off., Washington D.C., p. 893.
Sekanina, Z.: 1978, *Icarus* (in press).
Smith, A.W.: 1929, in *International Critical Tables*, Vol. V., p. 138.
Washburn, E. W.: 1928, in *International Critical Tables*, Vol. III, p. 210.
Watson, K., Murray, B. C. and Brown, H.: 1963. *Icarus* **1**, 317.
Weissman, P. R.: 1977a, *Bull. Amer. Astron. Soc.* **9**, 465.
Weissman, P. R.: 1977b, in A. H. Delsemme (ed.), *Comets, Asteroids and Meteorites*, University of Toledo Press, Toledo, p. 15.
Weissman, P. R.: 1978, IAU Symposium 81 (in press).
Whipple, F. L. and Sekanina, Z.: 1978, *Bull. Amer. Astron. Soc.* **10**, 589.
Yegibekov, P.: 1969, *Astrometriya i Astrofizika* **4**, 203, as translated in NASA TTF 599, p. 179.
Yeomans, D. K.: 1978, *Bull. Amer. Astron. Soc.* **10**, 590.